applied sciences

MDPI

Article

Machine-Learning-Based Elderly Stroke Monitoring System Using Electroencephalography Vital Signals

Yoon-A Choi [1], Sejin Park [2], Jong-Arm Jun [1], Chee Meng Benjamin Ho [3], Cheol-Sig Pyo [1], Hansung Lee [4] and Jaehak Yu [1,*]

[1] Department of KSB Convergence Research, Electronics and Telecommunications Research Institute (ETRI), Daejeon 34129, Korea; cyai@etri.re.kr (Y.-AC.); jajun@etri.re.kr (J.-A.J.); cspyo@etri.re.kr (C.-S.P.)
[2] Research Team for Health & Safety Convergence, Korea Research Institute of Standards and Science (KRISS), Daejeon 34113, Korea; sjpark6840@etri.re.kr
[3] AI Research Team, Sewon Intelligence Company, 35 Sejong-daero, Jung-gu, Seoul 04512, Korea; hocmb@sewon3h.com
[4] School of Computer Engineering, Youngsan University, 288 Junam-Ro, Yangsan, Gyeongnam 50510, Korea; mohan@korea.ac.kr
* Correspondence: dbzzang@etri.re.kr; Tel.: +82-42-860-6794

Abstract: Stroke is the third highest cause of death worldwide after cancer and heart disease, and the number of stroke diseases due to aging is set to at least triple by 2030. As the top three causes of death worldwide are all related to chronic disease, the importance of healthcare is increasing even more. Models that can predict real-time health conditions and diseases using various healthcare services are attracting increasing attention. Most diagnosis and prediction methods of stroke for the elderly involve imaging techniques such as magnetic resonance imaging (MRI). It is difficult to rapidly and accurately diagnose and predict stroke diseases due to the long testing times and high costs associated with MRI. Thus, in this paper, we design and implement a health monitoring system that can predict the precursors of stroke diseases in the elderly in real time during daily walking. First, raw electroencephalography (EEG) data from six channels were preprocessed via Fast Fourier Transform (FFT). The raw EEG power values were then extracted from the raw spectra: alpha (α), beta (β), gamma (γ), delta (δ), and theta (θ) as well as the low β, high β, and θ to β ratio, respectively. The experiments in this paper confirm that the important features of EEG biometric signals alone during walking can accurately determine stroke precursors and occurrence in the elderly with more than 90% accuracy. Further, the Random Forest algorithm with quartiles and Z-score normalization validates the clinical significance and performance of the system proposed in this paper with a 92.51% stroke prediction accuracy. The proposed system can be implemented at a low cost, and it can be applied for early disease detection and prediction using the precursor symptoms of real-time stroke. Furthermore, it is expected that it will be able to detect other diseases such as cancer and heart disease in the future.

Keywords: electroencephalography; machine learning; stroke prediction; real-time health monitoring; stroke disease analysis

Citation: Choi, Y.-A; Park, S.; Jun, J.-A.; Ho, C.M.B.; Pyo, C.-S.; Lee, H.; Yu, J. Machine-Learning-Based Elderly Stroke Monitoring System Using Electroencephalography Vital Signals. *Appl. Sci.* **2021**, *11*, 1761. https://doi.org/10.3390/app11041761

Academic Editor: José Ignacio Serrano
Received: 30 January 2021
Accepted: 12 February 2021
Published: 17 February 2021

1. Introduction

Stroke is a disease in which the blood vessels of the brain are blocked or have burst, thus resulting in sudden brain dysfunction such as motor or sensory disorders, pronunciation disorders, unconsciousness, or limb paralysis [1,2]. Strokes can be divided into two categories: cerebral infarction caused by large blockage of the blood vessels or cerebral hemorrhage caused by blood vessels bursting [3]. Cerebral infarction occurs when clots from the heart and carotid arteries (arteriosclerosis) eventually clog the cerebral blood vessels, while brain hemorrhages are marked by hemorrhages in the cerebral cortex and

intraventricular hemorrhage. Cerebral hemorrhage occurs spontaneously without any external shock, and high blood pressure is reported as its main cause [4]. Stroke disease is one of the most common severe disorders that causes functional disabilities in adults and older people, which can lead to substantial difficulties with social or economic activities [5–8]. For stroke patients, it is important to assess the current level of disability and to implement proper rehabilitation visits to medical institutions [9]. However, it is hard to classify stroke symptoms, making it difficult to properly diagnose disorders caused by stroke and any accompanying neurological damage. Therefore, there is a desperate need for technology that can keep track of potential stroke victims and support them during visits to medical institutions and allow them to receive diagnoses and treatments from medical staff as soon as possible.

Current research is attempting to identify major risk factors for stroke by evaluating the initial disability of stroke patients and monitoring their conditions [10,11]. Various methods for preventing the recurrence of these early disorders in stroke patients have been developed and studied, the Canadian Neurologic Scale and the National Institutes of Health Stroke Scale (NIHSS) are some of the scales used to diagnose the severity of stroke. In particular, the NIHSS developed by Lyden et al. is used as a measurement that is relatively easy and simple to perform at the beginning of hospitalization [12]. It is a proven tool used widely throughout the world. Based on various studies for reliability and feasibility, 14 key categories have been chosen for evaluation by the medical staff for the NIHSS: consciousness level, facial paralysis, vision, upper and lower extremism, distal motion, limb motion, hearing impairment, and sensory touch. Although it only takes about six minutes to evaluate a patient according to the NIHSS, it has the limitation of not providing accurate predictive information results for the early detection of stroke or initial disability [12].

A study by Jee et al. established a predictive model of stroke occurrence for Koreans [13]. Based on health examination data from the Korea National Health Insurance Corporation, Jee et al. developed 10 year prediction models for the average risk of stroke using age, diabetes, smoking, total cholesterol, drinking volume, systolic blood pressure, exercise, and body mass index (BMI). However, that study follows the same method as the construction of the stroke risk prediction model by the Framingham Heart Study [14]. It is important to know what type of stroke (brain infarction, cerebral hemorrhage) has occurred and how much damage the brain has taken within three hours of the stroke outbreak [15]. Based on these risk factors, studies have attempted to predict stroke diseases using various statistical methods and machine-learning methods; these include research using logistic models such as Kannel [16] and studies based on Cox's proportional risk model [14] and the Weibull model [17]. However, it is difficult to apply these risk-based models to predict the occurrence of stroke diseases in Koreans. Therefore, there is a need to find a new model for stroke prediction that is appropriate for the elderly in Korea. In addition, clinical studies have reported that stroke recurrence rates vary depending on the type of stroke and risk factors, but the typical recurrence rate within a year is 10–15% [18]. Therefore, it is important to quickly predict the early onset in stroke patients and those with a stroke history.

In this paper, we propose a health monitoring system that enables the real-time early detection of stroke and other diseases in older people based on EEG vital signals collected during daily activities. To accurately predict and to analyze the stroke disease, studies based on information on the features and patterns of EEG are being actively conducted [19,20]. In this paper, important features in EEG vital signals were newly defined and used in experiments. Specifically, raw EEG biometric signals data from elderly people aged 65 or older were collected during walking and stored in real time. These real-time raw EEG data were preprocessed with decomposing functions or frequency components via Fast Fourier Transform (FFT). The extracted raw spectrum includes alpha (α), beta (β), gamma (γ), delta (δ), theta (θ), low β, high β, and θ to β ratio, each taken from six measurement locations (Fz, Oz, T7, T8, C1, and C2), meaning 66 important attributes were used in total.

Our experiments have shown that the chosen attributes collected in real time while the elderly were walking can help detect and determine the precursor symptoms of more than 90% of stroke diseases in advance. Further, the Random Forest algorithm-based prediction model for stroke conditions with quartiles and a Z-score was experimentally identified with performance indicators such as accuracy and recall, preservation, and an F1-score of up to 92.51%. Thus, we present in-depth analysis results obtained through the performance and semantic interpretation of the elderly disease prediction and health monitoring system proposed in this paper, which are significant. Our initial results confirm that the proposed health monitoring system is able to detect and predict stroke precursors for older people in real time, and that it can be implemented at a low cost.

The remaining parts of this paper are organized as follows. In Section 2, we provide the literature review of the methodology involved in stroke diseases using EEG and machine learning. The elderly health monitoring system based on a machine-learning prediction model that collects real-time EEG vital signals is proposed in Section 3. Section 4 details the experimental results and presents an in-depth analysis of this paper, and finally, Section 5 discusses the conclusions and future research.

2. Related Works

Electroencephalography (EEG) is a human physiological signal that measures human brain waves [19–21]. Most of the studies utilizing EEG data have used them to identify and analyze epilepsy diseases, but reports of unique brain waves have recently been found in other diseases, including schizophrenia, depression, and stroke [11,21,22]. Beyond the raw EEG spectrum, prior research has shown that the absolute power value, which is the value of the attribute depending on the frequency domain, and the relative power value, which represents the ratio of the total amplitude at the frequency band, are better indicators for determining brain dysfunction [22]. Relative power is based on the ratio of the total amplitude of the frequency band, independent of the electrical resistance to the skull thickness and other non-brain wave electrical activity. Thus, each signal can vary depending on the reader's noise screening ability, ability to compare absolute power with relative power, understanding of psychoanalysis, and neurological knowledge [23,24]. Many studies have attempted to classify and predict various brain diseases using EEG data [25–32]; these have included studies on brain function location [25,26] as well as analyses of brain wave changes with human emotion [27,28] and brain wave changes with sleep level [29–31]. There have also been a number of studies predicting brain diseases using various frequency attribute values, such as absolute power values or relative power values [22]. For example, there have been studies attempting to automatically classify or predict patients with epilepsy [31], detect and diagnose depression [32], and detect early Alzheimer's conditions [33]. Further, the environments required of vital-signal collection methods, including EEG, limit such methods to studies based on data collected through medical equipment, such as large hospitals, rather than data collected from the daily activities of the elderly.

Several studies have reported the appearance of certain attribute values in stroke patients with EEG-based stroke analysis [34–37]. For example, Simon et al. [34] confirmed that the main properties of EEG with respect to stroke include the generation of abnormal and slow signals generated at the delta wave (δ) wave frequency range (1–4 Hz) with the simultaneous reductions of normal and fast activities at the alpha (α) wave frequency range (8–12 Hz). Through these experiments, we can confirm that relative delta power, delta and alpha power ratio, and the addition of delta and theta wave against alpha and beta wave ratios can be used to detect and predict stroke. Schneider et al. [35] studied EEG frequency analysis and topographic maps and found an increase in large delta waves and a decrease in alpha wave activity in 17 out of 20 mild stroke patients. Panayiotis et al. [36] confirmed that a rhythmic and high amplitude theta versus delta wave appeared in a patient with epilepsy during a stroke. Ip et al. [37] confirmed that brain waves in stroke patients that were measured in the cerebral cortex affected the activity and stability of the theta wave

and the delta wave, while the delta wave (0.1–3 Hz), alpha (7–13 Hz), beta wave (13–30 Hz), and high gamma wave (62–200 Hz) increased rapidly in the right hemisphere. Based on these studies, we believe that EEG research can help minimize medical costs and enable the early detection stroke diseases in the elderly during their daily activities.

A quick literature review found a few studies using various machine-learning techniques, including artificial neural networks (ANN), for stroke diagnosis or prediction [38–42]. For example, Shanthi et al. [38] reported that an individual's risk rate for stroke can be detected using ANN based on stroke patient data. Specifically, they used the backpropagation algorithm for learning, and showed improvements in consistency and diagnostic accuracy for the prediction. Nwosu et al. [39] studied the analysis and prediction of risk factors associated with the onset of stroke using data mining techniques and individual patient electronic health records. According to the experimental results, the prediction accuracy of decision tree (DT) was 74.31%, Random Forest was 74.53%, and ANN algorithm was 75.02%. Bentley et al. [40] reported a prediction method considering CT information and clinical variables in the treatment of ischemic stroke. Based on computed tomography (CT) images of 116 ischemic stroke patients, they successfully found 9 out of 16 patients with hemorrhage symptoms using support vector machines (SVMs). Hanifa et al. [41] predicted and verified the risk factors of stroke by adjusting the parameter values of the SVM prediction model using various kernel functions. Yu et al. [42] published a study detailing a prior detection and prediction methodology for stroke diseases with machine-learning and deep-learning methodologies by collecting electromyography (EMG) biological signals from thighs and calves in real time. More specifically, they measured and collected EMG data from the left and right thighs and the calves at 1500 Hz from the healthcare device. Using those data, they achieved over 90% stroke disease prediction accuracy.

Yu et al. [43,44] published an analytical study based on the decision tree methodology, which is a representative classification model of machine learning or data mining. In addition, Yu et al. [44] attempted to implement automatic classification and interpretation of the severity of NIHSS based on the C4.5 decision tree algorithm. By analyzing the rules on the additional operating principles provided by C4.5 decision trees, they were able to develop a novel attempt at the semantic interpretation of stroke severity. However, decision trees are predictive model algorithms by nature, which only provide partial interpretations, thus requiring in-depth analysis inherent in the data. In addition, Amini et al. [45] conducted a study to predict stroke outbreaks based on abundant medical data on a wide range of diseases. However, such research methodologies, like prior studies, are not suitable for use in early prediction models of stroke symptoms in real time in everyday life. Because these strokes interact with various risk factors rather than with one factor, studies of stroke disease prediction using various statistical methods and machine-learning methods are needed, and they are actively underway.

3. Elderly Stroke Monitoring System Based on Machine Learning and EEG

For the elderly stroke monitoring system, information on the important attributes was extracted from the raw data of EEG collected from six channels. After collecting and analyzing real-time EEG data, we proposed a monitoring system that can make early predictions of stroke and diseases in the elderly. The structure of the proposed system is presented in Figure 1 and includes (1) the EEG sensor and transmission module that collects and transmits the vital signals; (2) a collection module that integrates and stores various real-time generated multi vital-signals collector units (MVCU) and transmits them to a server; (3) a storage module that filters and stores the EEG information; and (4) the proposed system collects various types of vital-signal data, including actual EEG from the elderly, undertakes a series of data preprocessing and critical attribute extractions, and applies machine-learning models to predict and analyze stroke precursors in real time.

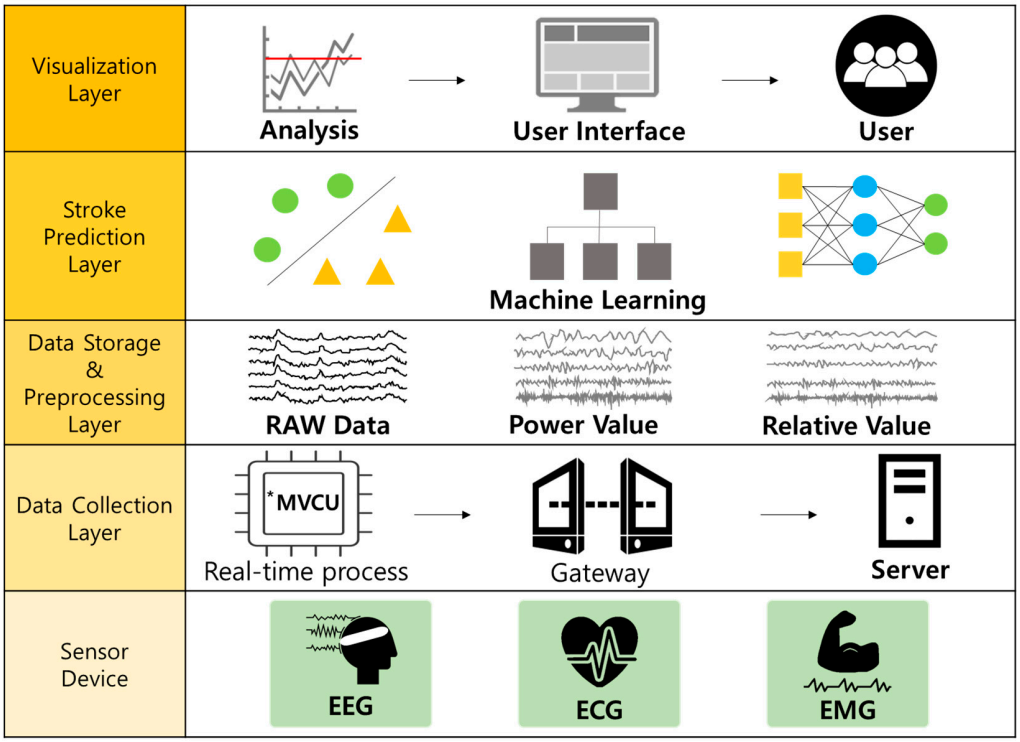

Figure 1. Elderly stroke monitoring system based on machine learning using electroencephalography (EEG). * MVCU: Multi Vital-Signals Collector Units.

3.1. Real-Time EEG Data Collection

This section describes the process used to measure and collect different types of biometric signal data, including EEG, ECG, EMG, pulse wave (PPG), and motion (motion), to validate the performance of the AI-based elderly stroke disease prediction and analysis system. Brain waves are the most basic electrical signals used to determine brain abnormalities, and they are measured through electrodes attached to the surface of the head. In this work, scalp EEG is used to measure and collect brain waves from the general elderly and stroke elderly patients. We hypothesize that these EEG vital-signal data can represent medical and kinematic parameters if the balance of the body collapses or if a walking disorder occurs during walking. The measurement and collection of the brainwave vital-signal data tested in this paper were conducted by the Emergency Medical Center and Rehabilitation Department of Chungnam National University Hospital for the elderly from 2017 to 2018. The subjects were aged 65 or older and had received rehabilitation treatment for stroke, since our focus is on elderly health monitoring. Various biometric signals, including EEG, ECG, EMG, voice, pulse, and motion, were collected using wearable sensors. To separate the general patients from the stroke patients, patients who had been diagnosed as a confirmed stroke case within one month were classified as stroke patients. The EEG data were collected at a sampling rate of 1000 Hz at a total of six channels (Fz, Oz, T7, T8, C1, and C2), with the location of each channel highlighted in Figure 2.

3.2. EEG Data Preprocessing

The data used in the experiments in this paper consist of three types: (1) raw EEG data collected from the brain wave measurement sensor; (2) absolute power value expressed by measuring absolute brain wave values regardless of external conditions such as scalp resistance, skull thickness, etc.; (3) relative power values to control for the difference in external states. The collected raw values that were imprecise were removed prior to learning, and a Z-score technique was applied on a channel-by-channel basis to complete the normalization process. The finalized data that had been preprocessed were then tailored to the input frame of the learning model. Finally, the number of selected EEG data stroke

patients used in the experiment was matched to the number of EEG data for the general elderly. Figure 3 below shows an example of the actual raw data values collected from six channels of brain waves measured and collected in real time. Figure 3a presents randomly selected EEG general elderly data and Figure 3b presents randomly selected stroke elderly data collected during walking.

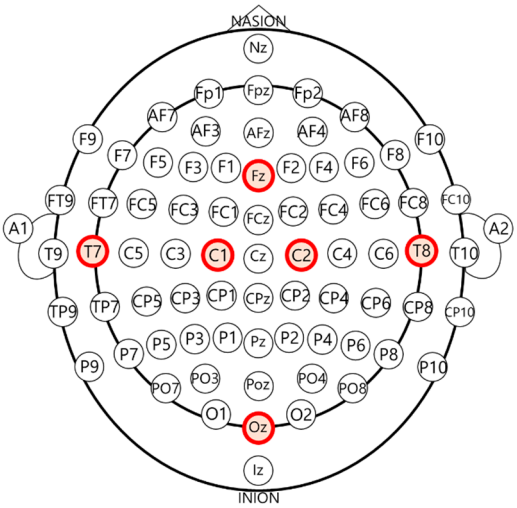

Figure 2. 6-channel measurement and collection locations of EEG vital signals.

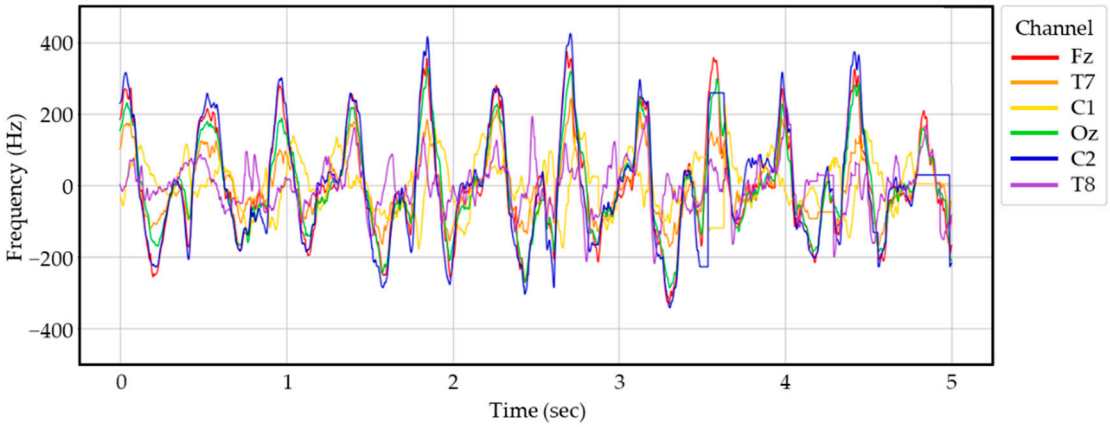

(**a**) Raw EEG signals from normal elderly patient.

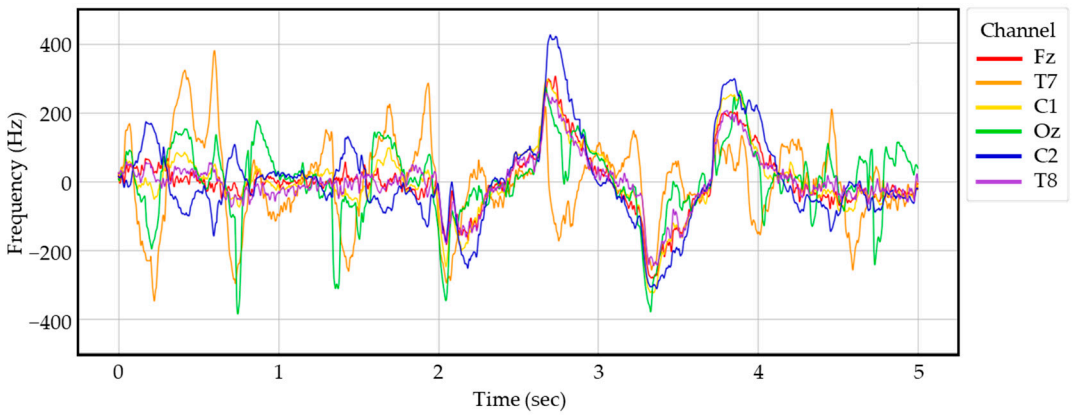

(**b**) Raw EEG signals from stroke elderly patient

Figure 3. Example of raw EEG vital-signals waveform changes while walking: (**a**) normal elderly patient, (**b**) stroke elderly patient.

In this paper, the absolute and relative power values collected from each subject were extracted and used. As the population of subjects is bound to have more general elderly people than stroke patients, the same amounts of data from stroke patients and randomly chosen general patients were selected; this was done to remove any form of bias in learning for stroke precursors and disease prediction.

3.3. Attribute Definition and Extraction in EEG

The experiments in this paper require raw data to be collected in the form of EEG signals during walking scenarios, as it does not use segment data from various experimental protocols. We conduct experimental and stroke disease prediction model studies by extracting the important properties from the raw values of these EEG signals. FFT was applied from the raw value of the EEG signal from each channel to extract the measurement variables raw spectrum alpha (α), beta (β), gamma (γ), delta (δ), and theta (θ), as well as the properties between the value's low β, high β, and theta-to-beta ratio. In this experiment, 66 attributes in total were newly defined and extracted in the form of the absolute power and relative values of waveforms (signals) from the raw EEG spectrum. The absolute power value and relative value used in the experiment in this paper consist of 11 attribute values for each of the six channels (Fz, Oz, T7, T8, C1, and C2), as listed in Table 1, which ultimately account for 66 attribute values and class.

Table 1. Detailed Descriptions of Newly Defined and Extracted EEG Attributes.

No. \ Contents	Features		Meaning and Explanation
1 ~ 66	6 Channel (Fz, Oz, T7, T8, C1, C2)	Delta (δ)	Delta power (1~4 Hz)
		Theta (θ)	Theta power (4~8 Hz)
		Alpha (α)	Alpha power (8~13 Hz)
		Beta (β)	Beta power (14~30 Hz)
		Gamma (γ)	Gamma power (30 Hz or more)
		Low_Beta	Low beta power (12~25 Hz)
		High_Beta	High beta power (25~30 Hz)
		Theta_to_Beta	Value of the beta ratio in theta (extracting abnormal theta waves)
		Delta divided by Alpha (DAR)	Ratio of mean power (Delta/Alpha)
		IDAR	Inverse ratio of DAR (Alpha/Delta)
		PRI	PRI power ratio index (delta+theta to alpha+beta), Low frequency to high frequency
67	Class Labeling		Normal or Stroke Elderly

Choosing an efficient subset of attributes for pattern classification is one of the most important research steps [46,47]. In this paper, we use the method described by Hall [48], which has already proven its performance in various fields of attribute subset selection for power and relative values of EEG. A merit function (Equation (1)) is used to evaluate how efficiently each subset of $F_s \subset F$ expresses the entire attributes. The subset with the largest value of the merit function is determined by the subset that best represents the entire property [48].

$$Merit(F_s) = \frac{k\overline{r_{cf}}}{\sqrt{k + k(k-1)\overline{r_{ff}}}} \quad (1)$$

where k is the number of attributes in subset F_s, $\overline{r_{cf}}$ is the mean distribution of attributes contained in F_s, and $\overline{r_{ff}}$ is the mean correlation value of the attributes. Tables 2 and 3 present the optimal subset of attributes chosen from absolute power value and relative

value using Hall's method. Table 2 lists a subset of eight attributes selected from the power value, and Table 3 lists a subset of 15 optimal attributes selected from the relative value.

Table 2. Optimal feature subset extracted from the power value of EEG.

No.	Features	Meaning and Explanation
1	Fz(Theta)	Theta power of Fz channel
2	Fz(Theta_to_Beta)	Beta ratio value in theta of Fz channel
3	Fz(IDAR)	Inverse ratio of DAR of Fz channel
4	Fz(RRI)	Power ratio index of Fz channel
5	T7(RRI)	Power ratio index of T7 channel
6	C1(DAR)	Ratio of mean power of C1 channel
7	Oz(IDAR)	Inverse ratio of DAR of Oz channel
8	T8(RRI)	Power ratio index of T8 channel

Table 3. Optimal feature subset extracted from the relative value of EEG.

No.	Features	Meaning and Explanation
1	Fz(Alpha)	Alpha power of Fz channel (8~13 Hz)
2	Fz(Beta)	Beta power of Fz channel (14~30 Hz)
3	Fz(Gamma)	Gamma power of Fz channel (30 Hz or more)
4	Fz(IDAR)	Inverse ratio of DAR of Fz channel
5	T7(Theta)	Theta power of T7 channel (4~8 Hz)
6	T7(Alpha)	Alpha power of T7 channel (8~13 Hz)
7	T7(Gamma)	Gamma power of T7 channel (30 Hz or more)
8	C1(Theta)	Theta power of C1 channel (4~8 Hz)
9	Oz(Beta)	Beta power of Oz channel (14~30 Hz)
10	Oz(Gamma)	Gamma power of Oz channel (30 Hz or more)
11	C2(Beta)	Beta power of C2 channel (14~30 Hz)
12	C2(Gamma)	Gamma power of C2 channel (30 Hz or more)
13	C2(Low_Beta)	Low beta power of C2 channel (12~25 Hz)
14	T8(Theta)	Theta power of T8 channel (4~8 Hz)
15	T8(Gamma)	Gamma power of T8 channel (30 Hz or more)

3.4. Stroke Prediction Module for the Elderly Based on Machine Learning

The module proposed in this paper uses real-time EEG biometric signals to detect and predict elderly stroke precursors in advance, and it consists of two submodules in total. The offline submodules provide predictive models via Machine-Learning (ML) Training, which performs machine-learning model-specific learning from the preprocessing of brainwave signals. Meanwhile, the online sub-module provides medical staff with the risk of stroke in older adults based on real-time EEG data as shown in Figure 4.

First, the offline module consists of a total of four sub-blocks: (1) the biometric repository stores various biological signals generated while the elderly participate in daily activities. For example, this block collects, stores, and manages EEGs, electrocardiograms (ECGs), pulse waves, and EMGs. (2) In the preprocessing of brain waves, the null and missing values of raw values collected in real time from the six channels are corrected or deleted. (3) Fast Fourier Transform (FFT) performs the task of decomposing functions or signals into frequency components, specifically by transforming the raw value of brain waves into individual spectral components. Next, the frequency information for the signal is extracted in real time. For example, alpha, beta, etc. are extracted, as shown in Table 2. Further, a learning model can be developed using both absolute power and relative values for 11 properties extracted per six channels. Finally, as presented in Tables 2 and 3, learning and prediction models are developed by selecting the optimal set of attributes used in real-time stroke disease prediction. (4) The machine-learning-based learning module implements learning based on attributes extracted from EEG biometric signals collected in real time. At this time, the prediction model learned from machine-learning algorithms in this block uses brainwave data from older people collected in real time during everyday activities. In

addition, the learned predictive model is passed to the online module so it can be used to determine the degree of precursors and predictions for stroke.

The online module also consists of a total of four sub-blocks: (1) Real-time data on brain waves are collected in the form of biological signals during everyday life, such as walking, from the elderly. (2) In the preprocessing of brain waves, corrections and noise data collected in real time during daily life are deleted. (3) Through FFT, the raw data values of each of the six channels of brain waves are decomposed into frequency components, and frequency information is extracted for the signal. (4) In the real-time stroke disease prediction block, the machine-learning-based learning module of the offline module uses a learned prediction model to make real-time predictions of elderly stroke disease using the incoming EEG data. Finally, the stroke disease prediction results and analysis information are delivered to the medical staff to be used as objective data for clinical treatment and diagnosis.

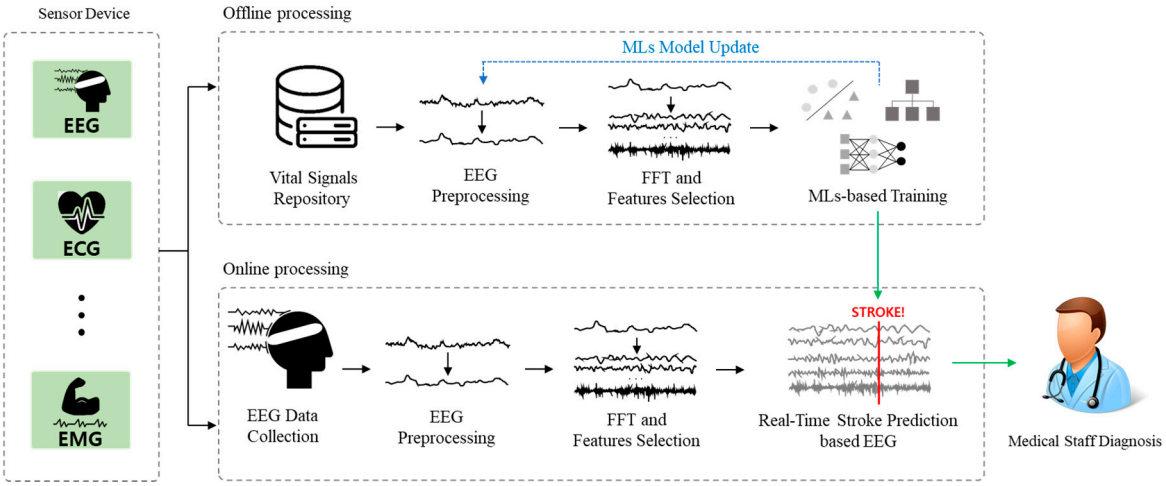

Figure 4. Overall structure of ML-based elderly stroke disease prediction module using real-time EEG vital signals.

4. Experiment and Analysis

4.1. Dataset and Experimental Environment

In this section, we describe the brain stroke precursor detection and disease prediction experiments that were conducted with older people on the previously described machine-learning models with raw value, power value, and relative value. We collected data on 48 stroke patients and 75 control patients in 2017, as well as 13 stroke patients and 137 control groups in 2018. For our experiments, all 61 stroke patients and a randomized selection of 61 patients from the control group were selected to balance the data from the stroke and control groups. In total, five scenario-specific measurement protocols were implemented, including walking, sleeping, moving objects, standing, and standing from a chair to stimulate the daily activities of an elderly person. The experiment was designed so that all subjects would go through one practice round before executing the measurement protocol according to each scenario. Despite the initial trial run, the first measured and collected values were not used as experimental data, because they could reflect human noise values stemming from the subject's tension and discomfort. The last fifth measurement protocol was also not reflected in the experimental data, because repeated experiments and fatigue were likely to be reflected in the data.

For the machine-learning-based experiments, we conducted stroke disease prediction experiments and analyze the data by extracting power and relative values based on raw values in the form of brain waves. We also experimented with the optimal set of attributes chosen using CFS (Correction Feature Selection) by power and relative values. The optimal subset of attributes from the power value is: Fz(θ), Fz(θ_to_β), Fz(*IDAR*), Fz(*RRI*), T7(*RRI*), C1(*DAR*), Oz(*IDAR*), T8(*RRI*), and the optimal set of attributes from the relative values

is: Fz(α), Fz(β), Fz(γ), Fz(*IDAR*), T7(θ), T7(α), T7(γ), C1(θ), Oz(β), Oz(γ), C2(β), C2(γ), C2(*Low_*β), T8(θ), and T8(γ). This combination of 23 attributes was used, and the algorithms of machine learning used in the experiment were Random forest, C4.5 decision tree, C5.0 decision tree, naive Bayes, MLP (multi-layer perceptron), logistic regression, two-class SVM (support vector machine), C&RT (classification and regression tree), and QUEST (quick unbiased efficient statistical tree).

4.2. Performance Evaluation Measurement

This section describes the statistical indicators used in disease screening to assess the system's performance in predicting strokes with EEG data, and the definitions of the performance evaluation indicators used are as follows (see Table 4) [47,49]. In this paper, we validate the performance of the system using four performance metrics, which are described in detail below. The misclassification of patients with stroke symptoms as normal elderly people can have a significant impact on their lives. Therefore, this misclassification is used as the most important performance evaluation indicator in health and medical services. As a result, it is important to find a model with high precision and high accuracy for stroke diseases in older people, while also having low false positives (FP).

Table 4. Confusion matrix of performance evaluation for prognostic symptoms and prediction of stroke.

		True Condition	
		Stroke Elderly	Normal Elderly
Predicted Condition	Stroke Elderly	True Positive	False Positive
	Normal Elderly	False Negative	True Negative

4.3. Experiment Based on Machine-Learning Methodology

This section extracts the power values, relative values from real-time EEG data, and machine-learning methods described in Section 3, Random Forest, C4.5 decision tree, C5.0 decoration tree, naive Bayes, logistic regression, MLP, and SVM-class. We learned and tested each machine-learning-based predictive model with power values and relative values, and we conducted our experiment and analysis based on eight optimal sets of attributes of power values using CFS (Correlation Feature Selection, Equation (1)).

4.3.1. Predicting and Analyzing Stroke Diseases Based on Power Values

In the first experiment, 2940 data sets were extracted and tested for the elderly and the elderly with stroke power values. To verify the performance of this model, we used the performance indicators defined in Section 4.2. Tables 5 and 6 below show the prediction accuracy and the performance indicators of F1-score, recall, and precision using all 66 attributes as well as different datasets per algorithm.

The second experiment performed a Z-score (normalization) for all 66 attributes. As an example of normalization application, it is necessary to prevent the patient-specific Oz_θ value from varying in category and size of the minimum and maximum values, since there are problems that can arise depending on the unit of measure. This normalization process translates the data so that they are within a small range of 0.0 to 1.0, so that the same weights are applied for all attributes.

$$\vec{x_i} = \frac{x_i - \mu}{\sigma} \times \alpha \quad (2)$$

In Equation (2), σ and μ are the standard deviation and mean of attribute x, respectively, and α is the weighted value, which is set as 1.0 in this paper. The proposed approach with Random Forest achieved over 91% in an accuracy, F1-score, Recall and Precision criteria. It also showed an accuracy of 92.52%, a F1-score of 92.5%, a recall of 92.5%, and a precision of 92.8% on the 10-fold CV dataset. It achieved over 90% in an accuracy, F1-score,

Recall and Precision criteria with MLP (ANN). It showed an accuracy of 90.83%, a F1-score of 90.8%, a recall of 90.8%, and a precision of 90.8% on the 10-fold CV dataset. Overall, it is confirmed that the performance was improved by 1% compared to the first experiment.

Table 5. Prediction accuracy and F1-score (%) for each algorithm using EEG power values.

Data Sets / Methods	Train (67)/ Test (33)		Train (80)/ Test (20)		5-Fold CV [1]		10-Fold CV		20-Fold CV	
	Acc. [2]	F1 [3]	Acc.	F1	Acc.	F1	Acc.	F1	Acc.	F1
RandomForest	92.37	92.4	91.92	91.9	90.66	90.6	90.95	90.9	91.07	91.1
C4.5 DT [4]	88.35	88.3	87.15	87.2	87.81	87.8	88.18	88.2	87.98	88.0
C5.0 DT	84.89	84.8	83.14	83.2	83.92	83.9	84.67	84.5	84.43	84.4
Naive Bayes	75.67	75.1	75.43	75.0	74.44	73.8	74.46	73.8	74.47	73.8
LR [5]	84.90	84.9	85.29	85.3	83.95	83.9	83.96	84.0	84.06	84.1
MLP(ANN) [6]	89.17	89.2	90.47	90.6	89.64	88.9	90.68	90.7	89.89	89.8
SVM	81.56	81.5	82.08	82.1	82.44	82.4	82.72	82.7	82.68	82.7
ADTree	85.63	85.6	86.82	86.8	88.86	88.9	89.91	89.9	89.66	89.7
C&RT	83.09	83.1	83.22	83.2	83.27	83.3	84.28	84.2	84.32	84.3
QUEST	78.57	78.6	77.92	77.9	78.36	78.4	79.72	79.7	79.59	79.6

[1] CV: Cross-Validation, [2] Acc.: Accuracy, [3] F1: F1-score, [4] DT: Decision Tree, [5] LR: Logistic Regression, [6] MLP: Multi-Layer Perceptron.

Table 6. Recall and Precision (%) for each algorithm using EEG power values.

Data Sets / Methods	Train (67)/ Test (33)		Train (80)/ Test (20)		5-Fold CV		10-Fold CV		20-Fold CV	
	Recall	Prec. [1]	Recall	Prec.	Recall	Prec.	Recall	Prec.	Recall	Prec.
RandomForest	92.4	92.6	91.9	92.1	90.7	90.9	91.0	91.2	91.1	91.3
C4.5 DT	88.4	88.4	87.2	87.2	87.8	87.8	88.2	88.2	88.0	88.0
C5.0 DT	84.9	84.9	83.2	83.1	83.9	83.9	84.7	84.6	84.4	84.4
Naive Bayes	75.7	78.7	75.4	78.5	74.4	77.1	74.5	77.2	74.5	77.2
LR	84.9	84.9	85.3	85.3	83.9	84.0	84.0	84.0	84.1	84.1
MLP(ANN)	89.2	89.2	90.5	90.7	88.9	89.4	90.7	90.7	89.8	89.9
SVM	81.6	81.5	82.1	82.1	82.4	82.3	82.7	82.6	82.6	82.7
ADTree	85.6	85.7	86.9	86.8	88.8	88.9	89.9	89.9	89.7	89.7
C&RT	83.1	83.1	83.2	83.2	83.3	83.3	84.3	84.2	84.3	84.3
QUEST	78.5	78.6	77.9	77.9	78.3	78.4	79.7	79.7	79.5	79.6

[1] Prec.: Precision.

In the following experiments, 36 properties were used, including brainwave information, such as δ and θ, which are clinically associated with prior studies as well as stroke analysis based on brainwaves. In addition, properties such as α, β, and γ were removed and used as experimental data. As with the previous experiments, each attribute was normalized using the Z-score method and tested with the resulting value. The random forest algorithm showed more than 91% performance index, and on the 10-fold CV dataset, the accuracy was 91.97%, F1-score 91.9%, recall 91.9%, and precision 92.9%. MLP showed relatively good performance with accuracy of 90.59%, F1-score 90.6%, recall 90.6%, and precision 90.7%. Other algorithms were verified through an experiment to show performance indicators of 80%. Comparing this experiment with the second experiment, it decreased

by about 1% in performance indicators including accuracy. However, by reducing the number of attributes used in the experiment by 36, the advantage of using less computing resources and an easier system operation in terms of the service of the stroke prediction model was obtained.

In the last experiment employing power values, the optimal set of attributes using Equation (1) is: Fz(θ), Fz(θ_to_β), Fz(*IDAR*), Fz(*RRI*), T7(*RRI*), C1(*DAR*), Oz(*IDAR*), and T8(*RRI*). Only eight were tested and analyzed for algorithm-specific predictive accuracy (see Table 2). Comprehensively examining the experimental results, most of the performance indicators were 80%. Regarding the Random Forest algorithm on the 10-fold CV dataset, the accuracy was 87.12%, F1-score 87.4%, recall 87.4%, and precision 87.4%, showing relatively good performance. The accuracy of the C4.5 DT algorithm was 86.39%, F1-score 85.79%, recall 86.4%, and precision 85.2%. Although the overall performance is inferior to the previous experiment, it could obtain the advantage of enabling semantic interpretation based on rule-based analysis and leaf node of decision tree. This semantic interpretation and in-depth analysis are explained in detail in Section 4.4.

4.3.2. Predicting and Analyzing Stroke Diseases Based on Relative Values

In the first experiment, 2979 data sets of the general elderly and the elderly with stroke were extracted and tested, respectively, with their relative values. Tables 7 and 8 below use 66 complete attributes and show prediction accuracy and performance indicators of F1-score, recall, and prescription by algorithm.

Table 7. Prediction accuracy and F1-score (%) for each algorithm using EEG relative values.

Data Sets / Methods	Train (67)/ Test (33)		Train (80)/ Test (20)		5-Fold CV		10-Fold CV		20-Fold CV	
	Acc.	F1	Acc.	F1	Acc.	F1	Acc.	F1	Acc.	F1
RandomForest	89.19	89.2	89.77	89.8	89.76	89.8	90.50	90.5	90.16	90.2
C4.5 DT	81.38	81.4	83.56	83.6	82.49	82.5	82.86	82.8	82.49	82.5
C5.0 DT	77.05	77.1	78.85	78.9	77.69	77.7	78.73	78.7	78.81	78.8
Naive Bayes	72.99	72.9	73.74	73.6	73.53	83.4	73.45	73.3	73.39	73.2
LR	78.54	78.5	79.11	79.1	78.70	78.7	78.68	78.7	78.60	78.6
MLP(ANN)	84.35	84.4	86.41	86.4	86.06	86.1	87.11	87.1	87.03	87.0
SVM	74.21	74.2	74.82	74.8	73.91	73.9	74.65	74.7	74.42	74.4
ADTree	79.91	79.9	79.36	79.4	79.33	79.3	79.48	79.5	79.31	79.3
C&RT	80.12	80.1	80.34	80.3	80.24	80.2	80.47	80.5	80.42	80.4
QUEST	73.88	73.9	73.91	73.9	73.55	73.6	73.94	73.7	73.75	73.8

In the second experiment, for all 66 attributes, the Z-score method (Equation (2)) of normalization was applied and these values were used for testing. In this experiment, Z-score was applied to the datasets used in Tables 7 and 8, and performance indicators ranged from 75% to 87% for each algorithm. In particular, regarding the Random Forest algorithm on the 10-fold CV dataset, the accuracy was 87.52%, F1-score 92.5%, recall 92.5%, and precision 92.8%, showing relatively good performance.

In the following experiments, 36 attributes, including brainwave information such as delta (δ) and theta (θ), which are highly associated with EEG-based stroke analysis and previous experiments, were normalized with Z-score methods and subsequently tested. In this experiment, performance indicators ranged from 72 to 85% for each algorithm. Similar to the previous experiment, regarding the Random Forest algorithm on the 20-fold CV dataset, the accuracy of 86.15%, F1-score 86.1%, recall 86.2%, and precision 86.2% were confirmed. On the other hand, regarding the SVM algorithm on the 5-fold CV dataset, the accuracy was 72.07%, F1-score 72.1%, recall 72.0%, and precision 72.3%. Compared to the

first experiment using the relative value, the overall performance index was lowered by 2%, but it was a meaningful experiment that could confirm relatively good performance index with only 36 of the 66 attributes.

Table 8. Recall and Precision (%) for each algorithm using EEG relative values.

Data Sets / Methods	Train (67)/ Test (33)		Train (80)/ Test (20)		5-Fold CV		10-Fold CV		20-Fold CV	
	Recall	Prec.	Recall	Prec.	Recall	Prec.	Recall	Prec.	Recall	Prec.
RandomForest	89.2	89.2	89.8	89.8	89.7	89.9	90.5	90.6	90.1	90.3
C4.5 DT	81.4	81.4	83.6	83.6	82.5	82.6	82.9	83.0	82.4	82.6
C5.0 DT	77.0	77.4	78.8	78.9	77.7	77.7	78.6	78.9	78.8	78.9
Naive Bayes	73.0	73.5	73.7	74.3	73.5	74.2	73.4	74.1	73.4	74.0
LR	78.5	78.5	79.1	79.1	78.7	78.7	78.7	78.7	78.6	78.6
MLP(ANN)	84.4	84.4	86.4	86.5	86.1	86.1	87.1	87.1	86.9	87.1
SVM	74.0	74.6	74.6	74.9	73.7	74.3	74.5	74.8	74.2	74.6
ADTree	79.9	80.0	79.2	79.5	79.2	79.4	79.5	79.6	79.1	79.4
C&RT	80.1	80.1	80.3	80.3	80.2	80.3	80.5	80.6	80.4	80.5
QUEST	73.9	73.9	73.9	73.9	73.4	73.7	73.8	73.9	73.5	73.9

In the final experiment of this section, we tested 15 optimal sets of attributes using Equation (1) in relative values: Fz(α), Fz(β), Fz(γ), Fz(*IDAR*), T7(θ), T7(α), T7(γ), C1(θ), Oz(β), Oz(γ), C2(β), C2(γ), C2(*Low_*β), T8(θ), and T8(γ). We conducted an experiment and analysis of predictive accuracy by algorithm (see Table 3). In this experiment, performance indicators ranged from 74 to 88% for each algorithm. In particular, when applying the Random Forest algorithm to the 20-fold CV dataset, the accuracy was 88.12%, F1-score 88.1%, recall 88.1%, and precision 88.6%. With the C4.5 DT algorithm, the performance of accuracy was 85.6%, F1-score 85.7%, recall 83.8%, and precision 87.7%. Compared to the previous experiment, the overall performance index was lower, but it was an experiment that could gain the advantage of enabling semantic interpretation of decision trees. These semantic interpretations and in-depth analysis are described in Section 4.4.

4.4. An In-Depth Analysis Based on the Power and Relative Features of EEG

In this section, we conduct a semantic analysis of stroke disease in the elderly using the power value of EEG based on the C4.5 algorithm among decision trees, a representative classification and prediction model of machine learning. In the first experiment, as a semantic analysis of the rules on predicting stroke conditions in older people, we randomly extracted and learned the power values of 2352 sets of data from both normal elderly and stroke patients, and we conducted testing with 588 data sets for normal elderly and stroke patients who did not participate in the learning. This section describes the experimental results of the C4.5 DT algorithm in the fourth experiment based on Equation (1) in Section 4.3.1. In the C4.5 DT algorithm, when 80% of train data and 20% of test data were applied, satisfactory prediction accuracy (86.39%), and stable performance of 86.4% for recall and precision was confirmed. Figure 5 shows a decision tree for predicting stroke conditions in the elderly with only eight attributes by applying the power value as CFS. In the construction of the decision trees, we showed that only eight of the 66 power value attributes defined by the system can be used to accurately classify and predict normal elderly and stroke patients. Here, the number in the leaf node is the corresponding class by learning data, which means the exact number of predictions and the number of incorrect predictions. Fourteen rules can be obtained from Figure 5. Summarizing Figure 5, the Fz channel values from the power values are analyzed as the main attributes. This was analyzed and confirmed by experiments indicating that the precursors for stroke disease

in older people were significant in the frontal lobe of the brain. Further, as shown in previous studies, attribute values such as θ_to_$\beta(\theta/\beta)$, PRI$(\delta+\theta)/(\alpha+\beta)$, and theta ($\theta$) are well identifiable and predictable for the characteristics of stroke patient brain waves.

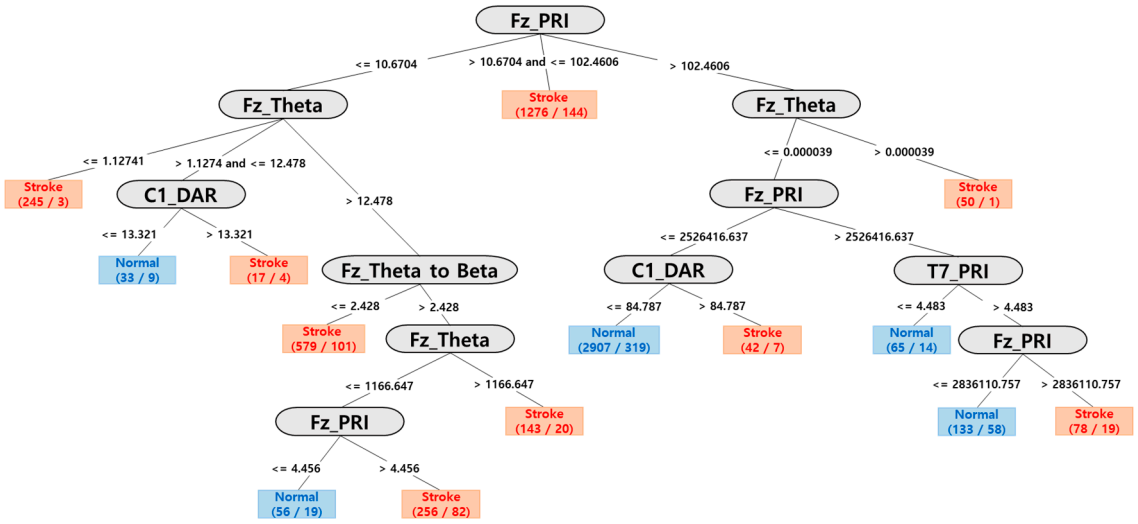

Figure 5. The C4.5 decision tree for elderly stroke prediction and monitoring based on power value (14 rules).

Figure 6 shows the experimental results of extracting eight attributes from the power values through the CFS and applying 10-fold CV. When compared to Figure 5, these experimental results suggest that stroke precursors in older people can be accurately predicted and determined by only seven rules. We showed the improvement in the prediction accuracy of stroke disease to 86.96%. A detailed interpretation of the seven rules in Figure 6 is presented in Table 9.

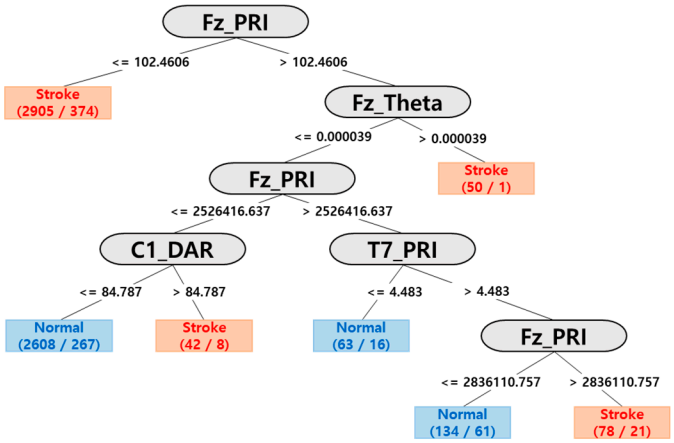

Figure 6. The C4.5 decision tree learning eight features of power value with 10-fold CV (7 rules).

A comprehensive analysis of Figure 6 and Table 9 above yields that the $PRI(\delta+\theta)/(\alpha+\beta)$ values in the frontal lobe are the most important attribute for classifying stroke brain signals, and that θ values are also used as important attributes.

The second experiment is the same as the first experimental scenario, and we proceed with relative values instead of power values. In other words, both experiments were conducted by dividing the data into 80% for the learning data and 20% for the test data, in Section 4.3.2, which achieve stable performances of 83.8% and 87.7%, respectively, in prediction accuracy (85.6%), along with reproducibility and precision. The performance indicators, including prediction accuracy, were slightly lower than those of the experiments with power values, but they were identified when relative values were used, and none

of the key attributes of power values were present. Figure 7 shows a decision tree for predicting stroke conditions in the elderly with only 15 attributes by applying the relative value as CFS. Experiments have shown that in the construction of decision trees, only 15 of the 66 relative value attributes defined by the system can accurately predict stroke precursors for normal and stroke elderly. Seventeen rules can be obtained from Figure 7.

Table 9. The rules for elderly stroke prediction with only eight features of 10-fold CV (Figure 6).

Rules	The Rule and In-Depth Analysis
1	IF Fz_PRI $\leq$ 102.4606 then Stroke.
2	IF Fz_PRI > 102.4606 and Fz_Theta $\leq$ 0.000039 and Fz_PRI $\leq$ 2,526,416.637 and C1_DAR $\leq$ 84.787 then Normal.
3	IF Fz_PRI > 102.4606 and Fz_Theta $\leq$ 0.000039 and Fz_PRI $\leq$ 2,526,416.637 and C1_DAR > 84.787 then Stroke.
4	IF Fz_PRI > 102.4606 and Fz_Theta $\leq$ 0.000039 and Fz_PRI > 2,526,416.637 and T7_PRI $\leq$ 4.483 then Normal.
5	IF Fz_PRI > 102.4606 and Fz_Theta $\leq$ 0.000039 and Fz_PRI > 2,526,416.637 and T7_PRI > 4.483 and Fz_PRI $\leq$ 2,836,110.757 then Normal.
6	IF Fz_PRI > 102.4606 and Fz_Theta $\leq$ 0.000039 and Fz_PRI > 2,526,416.637 and T7_PRI > 4.483 and Fz_PRI > 2,836,110.757 then Stroke.
7	IF Fz_PRI > 102.4606 and Fz_Theta > 0.000039 then Stroke.

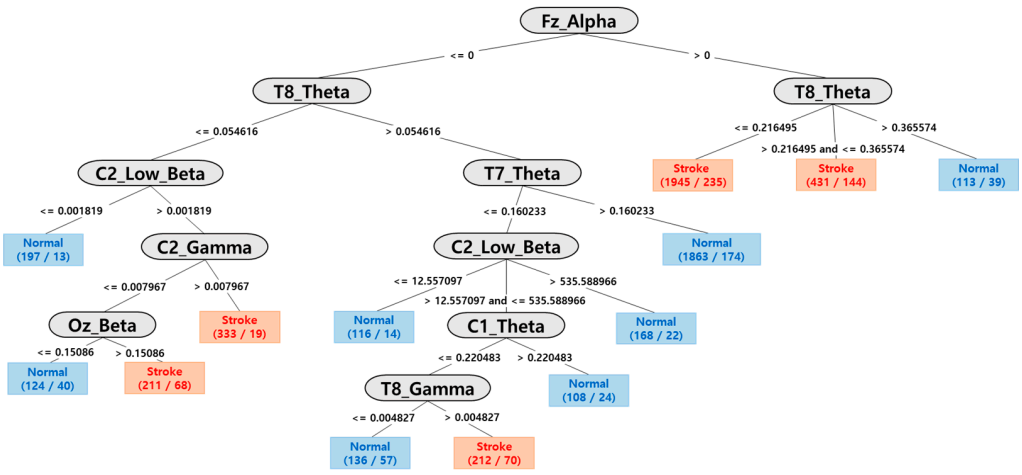

Figure 7. The C4.5 decision tree for elderly stroke prediction and monitoring based on relative value (17 rules).

Figure 8 shows the experimental results of extracting 15 key attributes via CFS from the relative values and applying 10-fold CV. These experimental results indicate that relative values can accurately predict and determine stroke precursors in older people with only 13 rules, as compared to the results illustrated in Figure 8. The predicted accuracy of stroke disease was 84.5%. By reducing and simplifying from 17 rules to 13 rules, the development and implementation of stroke monitoring systems for the elderly can help.

In a comprehensive analysis of the experiments using relative value, the properties of Fz channels corresponding to the frontal lobe, as shown in power values, are considered to be important properties for predicting stroke precursors in older people. However, the relative value data confirmed that the alpha (α) property of the Fz channel, which was not used in deep analysis using power values, was a significant value for determining and predicting the precursor symptoms of stroke. Further, through an in-depth analysis using relative value, we experimentally validate that not only Fz, but also attribute values for measurement positions such as T8, C2, and T7, are meaningful. Specifically, the analysis based on attributes extracted from relative value showed that θ_to_β(θ/β) and PRI(δ+θ)/(α+β) utilized in experiments employing power value were not used. As a

result, the experimental and in-depth analysis results showed that the entire portion of the brainwave measurement location is evenly utilized in the prediction of stroke precursors in older people using the attribute value of relative value.

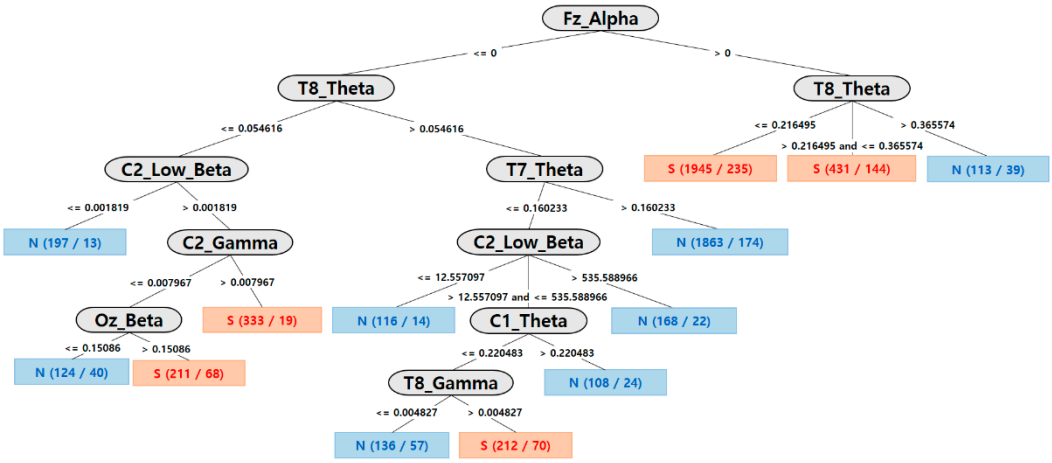

Figure 8. The C4.5 decision tree learning eight features of relative value with 10-fold CV (13 rules).

5. Conclusions

We propose a new health monitoring system that detects and predicts the precursor symptoms of stroke diseases with the attribute information of power and relative values from raw data in the form of brain waves collected during elderly walking. Further, the prediction and analysis model in machine-learning attempts to analyze the results of real-time predictions and experiments of stroke disease in older people. In addition, to generalize machine-learning-based predictive models, the measurement positions are diversified to extract raw spectra, raw spectrum, alpha (α), beta (β), gamma (γ), delta (δ), and theta (θ) values from six channels (Fz, Oz, T7, T8, C1, and C2) as well as low β and high β. By extracting additional ratio values between θ and β, 66 new attributes were ultimately discovered and tested. Above all, the health monitoring system in this study can detect and predict the precursors of stroke, a fatal disease for elderly people, in real time, thus providing accurate prediction results in a system that can be implemented at a low cost. This is an important experimental result that can detect the possibility of an outbreak of stroke disease early and provide scientific rules that can interpret it. As a result, the system in this study has great advantages, as it can provide in-depth analysis information useful for older patients, particularly about everyday activities such as walking. Thus, the proposed system and experimental results in this paper imply that they are meaningful findings that can reduce the aftereffects of stroke as well as social and economic losses.

In the future, research on stroke and other important diseases in the elderly should be conducted based on various real-time biological signals such as ECG and EMG as well as EEG. We will also study the prediction of precursors and outbreaks by disease and conduct in-depth analyses. We believe this will be a significant step toward developing more reliable and clinically useful health and disease prediction methods such as cancer and heart disease for the elderly through multimodal studies combining various vital signals, individual-specific electronic medical recording (EMR) data, and image information such as CT and MRI information.

Author Contributions: Conceptualization, Y.-AC. and J.Y.; methodology, Y.-AC., S.P., J.-A.J., C.M.B.H., C.-S.P., H.L. and J.Y.; software, Y.-AC. and J.Y.; validation, Y.-AC., S.P., J.-A.J., C.M.B.H., C.-S.P., H.L. and J.Y.; formal analysis, Y.-AC. and J.Y.; investigation, Y.-AC., S.P., J.-A.J., C.M.B.H., C.-S.P., H.L. and J.Y.; resources, Y.-AC. and J.Y.; data curation, Y.-AC. and J.Y.; writing—original draft preparation, Y.-AC., S.P., J.-A.J., C.M.B.H., C.-S.P., H.L. and J.Y.; writing—review and editing, Y.-AC., H.L. and J.Y.; visualization, Y.-AC. and J.Y.; supervision, J.Y and C.-S.P.; project administration, C.-S.P.; funding acquisition, C.-S.P. All authors have read and agreed to the published version of the manuscript.

Funding: This work was supported by the National Research Council of Science & Technology (NST) grant by the Korea government (MSIP) (No. CRC-15-05-ETRI).

Institutional Review Board Statement: This paper was researched after review and approval by KRISS-IRB (Institutional Bioethics Committee of Korea Research Institute of Standards and Science).

Informed Consent Statement: Informed consent was obtained from all subjects involved in the study.

Conflicts of Interest: The authors declare no conflict of interest.

References

1. Seo, K.-D.; Kang, M.J.; Kim, G.S.; Lee, J.H.; Suh, S.H.; Lee, K.-Y. National Trends in Clinical Outcomes of Endovascular Therapy for Ischemic Stroke in South Korea between 2008 and 2016. *J. Stroke* **2020**, *22*, 412–415. [CrossRef]
2. Mackay, J.; Mensah, G.A. *The Atlas of Heart Disease and Stroke*; World Health Organization: Geneva, Switzerland, 2004; pp. 22–43.
3. Kim, J.Y.; Bae, H.-J. Spontaneous Intracerebral Hemorrhage: Management. *J. Stroke* **2017**, *19*, 28–39. [CrossRef] [PubMed]
4. Johansson, B.B. Hypertension Mechanisms Causing Stroke. *Clin. Exp. Pharmacol. Physiol.* **1999**, *26*, 563–565. [CrossRef] [PubMed]
5. Gottesman, R.F.; Hillis, A.E. Predictors and assessment of cognitive dysfunction resulting from ischaemic stroke. *Lancet Neurol.* **2010**, *9*, 895–905. [CrossRef]
6. Korpelainen, J.T.; Kauhanen, M.-L.; Kemola, H.; Malinen, U.; Myllylä, V.V. Sexual dysfunction in stroke patients. *Acta Neurol. Scand.* **1998**, *98*, 400–405. [CrossRef]
7. Pikija, S.; Trkulja, V.; Ramesmayer, C.; Mutzenbach, J.S.; Killer-Oberpfalzer, M.; Hecker, C.; Bubel, N.; Füssel, M.U.; Sellner, J. Higher Blood Pressure during Endovascular Thrombectomy in Anterior Circulation Stroke Is Associated with Better Outcomes. *J. Stroke* **2018**, *20*, 373–384. [CrossRef]
8. Boden-Albala, B.; Litwak, E.; Elkind, M.; Rundek, T.; Sacco, R.L. Social isolation and outcomes post stroke. *Neurology* **2005**, *64*, 1888–1892. [CrossRef]
9. Langhorne, P.; Bernhardt, J.; Kwakkel, G. Stroke rehabilitation. *Lancet* **2011**, *377*, 1693–1702. [CrossRef]
10. Bushnell, C.D.; Johnston, D.C.; Goldstein, L.B. Retrospective assessment of initial stroke severity: Comparison of the NIH stroke scale and the Canadian neurological scale. *Stroke* **2001**, *32*, 656–660. [CrossRef]
11. Lee, M.; Ryu, J.; Kim, D. Automated epileptic seizure waveform detection method based on the feature of the mean slope of wavelet coefficient counts using a hidden Markov model and EEG signals. *ETRI J.* **2020**, *42*, 217–229. [CrossRef]
12. Lyden, P.; Brott, T.; Tilley, B.; Welch, K.M.; Mascha, E.J.; Levine, S.; Haley, E.C.; Grotta, J.; Marler, J. Improved reliability of the NIH Stroke Scale using video training. NINDS TPA Stroke Study Group. *Stroke* **1994**, *25*, 2220–2226. [CrossRef]
13. Lee, J.S.; Park, J.M.; Park, T.H.; Lee, K.B.; Lee, S.J.; Cho, Y.J.; Lee, J.Y. Development of a stroke prediction model for Korean. *J. Korean Neurol. Assoc.* **2010**, *28*, 13–21.
14. D'Agostino, R.B.; A Wolf, P.; Belanger, A.J.; Kannel, W.B. Stroke risk profile: Adjustment for antihypertensive medication. The Framingham Study. *Stroke* **1994**, *25*, 40–43. [CrossRef]
15. Musuka, T.D.; Wilton, S.B.; Traboulsi, M.; Hill, M.D. Diagnosis and management of acute ischemic stroke: Speed is critical. *Can. Med Assoc. J.* **2015**, *187*, 887–893. [CrossRef] [PubMed]
16. Kannel, W.; McGee, D.; Castelli, W. Latest perspectives on cigarette smoking and cardiovascular disease: The Framingham Study. *J. Card. Rehabil.* **1984**, *4*, 267–277.
17. Carroll, K.J. On the use and utility of the Weibull model in the analysis of survival data. *Control. Clin. Trials* **2003**, *24*, 682–701. [CrossRef]
18. Zhang, J.; Zhu, P.; Liu, B.; Yao, Q.; Yan, K.; Zheng, Q.; Li, Y.; Zhang, L.; Li, M.; Wang, J.; et al. Time to recurrence after first-ever ischaemic stroke within 3 years and its risk factors in Chinese population: A prospective cohort study. *BMJ Open* **2019**, *9*, e032087. [CrossRef] [PubMed]
19. Cicioğlu, M.; Çalhan, A. SDN-based wireless body area network routing algorithm for healthcare architecture. *ETRI J.* **2019**, *41*, 452–464. [CrossRef]
20. Subasi, A.; Alkan, A.; Koklukaya, E.; Kiymik, M.K. Wavelet neural network classification of EEG signals by using AR model with MLE preprocessing. *Neural Netw.* **2005**, *18*, 985–997. [CrossRef]
21. Guler, I.; Ubeyli, E.D. Multiclass Support Vector Machines for EEG-Signals Classification. *IEEE Trans. Inf. Technol. Biomed.* **2007**, *11*, 117–126. [CrossRef] [PubMed]
22. Rim, B.; Sung, N.-J.; Min, S.; Hong, M. Deep Learning in Physiological Signal Data: A Survey. *Sensors* **2020**, *20*, 969. [CrossRef]

23. Williams, G.W.; Lüders, H.O.; Brickner, A.; Goormastic, M.; Klass, D.W. Interobserver variability in EEG interpretation. *Neurology* **1985**, *35*, 1714. [CrossRef] [PubMed]
24. Benbadis, S.R.; Lafrance, W.C.; Papandonatos, G.D.; Korabathina, K.; Lin, K.; Kraemer, H.C.; Workshop, F.T.N.T. Interrater reliability of EEG-video monitoring. *Neurology* **2009**, *73*, 843–846. [CrossRef] [PubMed]
25. Toraman, S.; Tuncer, S.A.; Balgetir, F. Is it possible to detect cerebral dominance via EEG signals by using deep learning? *Med Hypotheses* **2019**, *131*, 109315. [CrossRef]
26. Sakhavi, S.; Guan, C.; Yan, S. Learning Temporal Information for Brain-Computer Interface Using Convolutional Neural Networks. *IEEE Trans. Neural Netw. Learn. Syst.* **2018**, *29*, 5619–5629. [CrossRef] [PubMed]
27. Kwon, Y.-H.; Shin, S.-B.; Kim, S.-D. Electroencephalography Based Fusion Two-Dimensional (2D)-Convolution Neural Networks (CNN) Model for Emotion Recognition System. *Sensors* **2018**, *18*, 1383. [CrossRef]
28. Bălan, O.; Moise, G.; Moldoveanu, A.; Leordeanu, M.; Moldoveanu, F. Fear Level Classification Based on Emotional Dimensions and Machine Learning Techniques. *Sensors* **2019**, *19*, 1738. [CrossRef]
29. Chambon, S.; Thorey, V.; Arnal, P.; Mignot, E.; Gramfort, A. DOSED: A deep learning approach to detect multiple sleep micro-events in EEG signal. *J. Neurosci. Methods* **2019**, *321*, 64–78. [CrossRef] [PubMed]
30. Acharya, R.; Faust, O.; Kannathal, N.; Chua, T.L.; Laxminarayan, S. Non-linear analysis of EEG signals at various sleep stages. *Comput. Methods Programs Biomed.* **2005**, *80*, 37–45. [CrossRef]
31. Tian, X.; Deng, Z.; Ying, W.; Choi, K.-S.; Wu, D.; Qin, B.; Wang, J.; Shen, H.; Wang, S. Deep Multi-View Feature Learning for EEG-Based Epileptic Seizure Detection. *IEEE Trans. Neural Syst. Rehabil. Eng.* **2019**, *27*, 1962–1972. [CrossRef]
32. Acharya, U.R.; Oh, S.L.; Hagiwara, Y.; Tan, J.H.; Adeli, H.; Subha, D.P. Automated EEG-based screening of depression using deep convolutional neural network. *Comput. Methods Programs Biomed.* **2018**, *161*, 103–113. [CrossRef]
33. Kim, D.; Kim, K. Detection of Early Stage Alzheimer's Disease using EEG Relative Power with Deep Neural Network. In Proceedings of the 2018 40th Annual International Conference of the IEEE Engineering in Medicine and Biology Society (EMBC), Honolulu, HI, USA, 18–21 July 2018; pp. 352–355.
34. Finnigan, S.; Wong, A.; Read, S.J. Defining abnormal slow EEG activity in acute ischaemic stroke: Delta/alpha ratio as an optimal QEEG index. *Clin. Neurophysiol.* **2016**, *127*, 1452–1459. [CrossRef] [PubMed]
35. Schneider, A.L.; Jordan, K.G. Regional Attenuation without Delta (RAWOD): A distinctive EEG pattern that can aid in the diagnosis and management of severe acute ischemic stroke. *Am. J. Electroneurodiagnostic Technol.* **2005**, *45*, 102–117. [CrossRef] [PubMed]
36. Varelas, P.N.; Hacein-Bey, L. Ischemic Stroke, Hyperperfusion Syndrome, Cerebral Sinus Thrombosis, and Critical Care Seizures. *Seizures Crit. Care* **2017**, *14*, 155–186. [CrossRef]
37. Ip, Z.; Rabiller, G.; He, J.W.; Yao, Z.; Akamatsu, Y.; Nishijima, Y.; Liu, J.; Yazdan-Shahmorad, A. Cortical stroke affects activity and stability of theta/delta states in remote hippocampal regions. In Proceedings of the 2019 41st Annual International Conference of the IEEE Engineering in Medicine and Biology Society (EMBC), Berlin, Germany, 23–27 July 2019; pp. 5225–5228.
38. Shanthi, D.; Sahoo, G.; Saravanan, N. Designing an artificial neural network model for the prediction of thrombo-embolic stroke. *Int. J. Biom. Bioinform.* **2009**, *3*, 10–18.
39. Nwosu, C.S.; Dev, S.; Bhardwaj, P.; Veeravalli, B.; John, D. Predicting Stroke from Electronic Health Records. In Proceedings of the 2019 41st Annual International Conference of the IEEE Engineering in Medicine and Biology Society (EMBC), Berlin, Germany, 23–27 July 2019; pp. 5704–5707.
40. Bentley, P.; Ganesalingam, J.; Jones, A.L.C.; Mahady, K.; Epton, S.; Rinne, P.; Sharma, P.; Halse, O.; Mehta, A.; Rueckert, D. Prediction of stroke thrombolysis outcome using CT brain machine learning. *NeuroImage Clin.* **2014**, *4*, 635–640. [CrossRef]
41. Hanifa, S.M.; Raja, S.K. Stroke risk prediction through non-linear support vector classification models. *Int. J. Adv. Res. Comput. Sci.* **2010**, *1*, 47–53.
42. Yu, J.; Park, S.; Kwon, S.-H.; Ho, C.M.B.; Pyo, C.-S.; Lee, H. AI-based Stroke Disease Prediction System Using Real-Time Electromyography Signals. *Appl. Sci.* **2020**, *10*, 6791. [CrossRef]
43. Yu, J.; Kim, D.; Park, H.; Chon, S.-C.; Cho, K.H.; Kim, S.-J.; Yu, S.; Park, S.; Hong, S. Semantic Analysis of NIH Stroke Scale using Machine Learning Techniques. In Proceedings of the International Conference on Platform Technology and Service (PlatCon), Jeju, Korea, 28–30 January 2019; Institute of Electrical and Electronics Engineers (IEEE): Piscataway, NJ, USA, 2019; pp. 1–5.
44. Yu, J.; Park, S.; Lee, H.; Pyo, C.-S.; Lee, Y.S. An Elderly Health Monitoring System Using Machine Learning and In-Depth Analysis Techniques on the NIH Stroke Scale. *Mathematics* **2020**, *8*, 1115. [CrossRef]
45. Amini, L.; Azarpazhouh, R.; Farzadfar, M.T.; Mousavi, S.A.; Jazaieri, F.; Khorvash, F.; Norouzi, R.; Toghianfar, N. Prediction and Control of Stroke by Data Mining. *Int. J. Prev. Med.* **2013**, *4*, S245–S249. [PubMed]
46. Oh, I.-S.; Lee, J.-S.; Moon, B.-R. Hybrid genetic algorithms for feature selection. *IEEE Trans. Pattern Anal. Mach. Intell.* **2004**, *26*, 1424–1437. [CrossRef] [PubMed]
47. Han, J.; Kamber, M.; Pei, J. *Data Mining: Concepts and Techniques*, 3rd ed.; Morgan Kaufmann: 225 Wyman Street, Waltham, MA 02451, USA, 2011.
48. Hall, M. Correlation-based Feature Selection for Machine Learning. Ph.D. Thesis, Deptartment of Computer Science, Waikato University, Hamilton, NZ, USA, 1998.
49. Grandini, M.; Bagli, E.; Visani, G. Metrics for multi-class classification: An overview. *arXiv* **2020**, arXiv:2008.05756.